Journal of Power Sources 256 (2014) 20–27

Contents lists available at ScienceDirect

Journal of Power Sources

journal homepage: www.elsevier.com/locate/jpowsour

An approach to application for $LiNi_{0.6}Co_{0.2}Mn_{0.2}O_2$ cathode material at high cutoff voltage by TiO_2 coating

Yanping Chen, Yun Zhang*, Baojun Chen, Zongyi Wang, Chao Lu

College of Materials Science and Engineering, Sichuan University, Chengdu, Sichuan 610065, PR China

HIGHLIGHTS

- Anatase nano-TiO_2 is successfully coated on the surface of $LiNi_{0.6}Co_{0.2}Mn_{0.2}O_2$.
- Appropriate amount of TiO_2 is beneficial to reduce cation disorder.
- The 1.0 wt.% TiO_2-coated $LiNi_{0.6}Co_{0.2}Mn_{0.2}O_2$ exhibits excellent electrochemistry properties.
- The TiO_2-coated $LiNi_{0.6}Co_{0.2}Mn_{0.2}O_2$ presents excellent thermal stability.

ARTICLE INFO

Article history:
Received 3 October 2013
Received in revised form
31 December 2013
Accepted 14 January 2014
Available online 23 January 2014

Keywords:
Nickel-rich cathode materials
Electrochemical performance
Anatase TiO_2 coating
High voltage
Lithium ion batteries

ABSTRACT

Nickel-rich $LiNi_{0.6}Co_{0.2}Mn_{0.2}O_2$ cathode material is coated with nano-sized anatase TiO_2 synthesized via hydrolyzation method to improve its electrochemical performance at high cutoff voltage of 4.5 V. Scanning electron microscopy (SEM), transmission electron microscope (TEM) and high resolution transmission electron microscope (HRTEM) results show that the anatase TiO_2 is successfully coated on the surface of $LiNi_{0.6}Co_{0.2}Mn_{0.2}O_2$ with nanoscale and the coating layer thickness is about 25–35 nm. X-ray diffraction (XRD) test results indicate that appropriate amount of TiO_2 coating is beneficial to form a good layered structure with less cation disorder. Charge–discharge test results demonstrate that the TiO_2-coated $LiNi_{0.6}Co_{0.2}Mn_{0.2}O_2$ presents excellent cycling capability, rate capability and thermal stability at cutoff voltage of 4.5 V. The 1.0 wt.% TiO_2-coated $LiNi_{0.6}Co_{0.2}Mn_{0.2}O_2$ exhibits a capacity retention of 88.7% after 50 cycles at 1 C and a discharge capacity of 135.8 mAh g^{-1} after 10 cycles at 5 C, comparing to those of the pristine $LiNi_{0.6}Co_{0.2}Mn_{0.2}O_2$ of only 78.1% and 85.4 mAh g^{-1}. Electrochemical impedance spectroscopy (EIS) and differential scanning calorimeter (DSC) tests results provide evidence that the improved electrochemical properties are mainly attributed to the suppression of the interface reaction between the cathode and electrolyte and the improvement of structural stability of the material by coating.

1. Introduction

Layered $LiNi_{1-x-y}Co_xMn_yO_2$ ($0 < x, y < 1$) cathode materials for lithium-ion batteries have been widely studied due to their higher capacity, excellent safety performance and lower cost compared with $LiCoO_2$ cathode materials [1–4]. Currently, $LiNi_{1/3}Co_{1/3}Mn_{1/3}O_2$ is considered to be one of the most promising cathode materials to replace the commonly used $LiCoO_2$ [5–7]. However, its capacity of 155 mAh g^{-1} is still too low to meet the ever-growing capacity needs, especially for electric vehicles (EVs) [8,9]. One approach to improve the discharge capacity of $LiNi_{1-x-y}Co_xMn_yO_2$ is to increase the content of Ni. So nickel-rich layered cathode materials, $LiNi_{1-x-y}Co_xMn_yO_2$ ($1 - x - y \geq 0.5$), have been investigated extensively [9–13]. Among the nickel-rich layered cathode materials, $LiNi_{0.6}Co_{0.2}Mn_{0.2}O_2$ has been expected to be a promising cathode material due to its comparatively better comprehensive electrochemical properties [2,10,14–17]. Unfortunately, the nickel-rich layered oxides, considered as a substitute material of $LiNiO_2$, still inherit many intrinsic disadvantages of $LiNiO_2$. The major problem associated with nickel-rich layered cathode materials includes the structural instability, the thermal instability at the fully charged state and the cycle instability. It is well known that the most critical factors for evaluating the performance of lithium-ion batteries are cycle life, rate capability, and thermal stability, which are mainly depended on the characteristics of the cathode materials. Therefore, there is no doubt that the commercialization of nickel-rich cathode materials is severely limited by their own deficiencies.

* Corresponding author. Tel./fax: +86 028 85410272.
E-mail address: y_zhang@scu.edu.cn (Y. Zhang).

0378-7753/$ – see front matter © 2014 Elsevier B.V. All rights reserved.
http://dx.doi.org/10.1016/j.jpowsour.2014.01.061

Furthermore, in the nickel-rich layered $LiNi_{1-x-y}Co_xMn_yO_2$ system, another approach to increase the reversible capacity is raising the upper cutoff voltage. This is also a main potential advantage for nickel-rich layered $LiNi_{1-x-y}Co_xMn_yO_2$ system comparing with $LiFePO_4$, $LiCoO_2$ or other system. However, the structural stability, cycle stability and thermal stability all will decrease at the same time [18,19]. The main reason is that the host structural degradation due to the reaction between the cathode material and the electrolyte, leading to the increase of the interfacial impedance [19,20].

In order to solve these problems, many efforts have been made to seek a feasible solution. Surface coating has been proved to be an effective method to improve the electrochemical performances and thermal stability of the cathode materials. Metal oxides or other materials such as Al_2O_3, ZrO_2, V_2O_5, ZnO, AlF_3, $Al(OH)_3$ and $AlPO_4$ [18–23] have been reported to be very effective coating materials. In addition, Wu et al. [7] reported the enhanced electrochemical performance of TiO_2-coated $LiNi_{1/3}Co_{1/3}Mn_{1/3}O_2$. Liu et al. [24] reported that the enhanced cycling stability was due to the fact that TiO_2 coating. To the best of our knowledge, there are no reports about the effect of anatase nano-TiO_2 coating on the nickel-rich layered $LiNi_{0.6}Co_{0.2}Mn_{0.2}O_2$ cathode materials, especially, at a high cutoff voltage of 4.5 V.

In this paper, anatase TiO_2 nanoparticles are coated on the surface of $LiNi_{0.6}Co_{0.2}Mn_{0.2}O_2$ via a hydrolyzation method. The effects of anatase TiO_2 coating on the structural and electrochemical performances of the $LiNi_{0.6}Co_{0.2}Mn_{0.2}O_2$ cathode materials in the high cutoff voltage (4.5 V) are investigated in detail.

2. Experimental

Firstly, $Ni_{0.6}Co_{0.2}Mn_{0.2}(OH)_2$ precursor was prepared by co-precipitation method. A stoichiometric amount of $NiSO_4 \cdot 6H_2O$, $CoSO_4 \cdot 6H_2O$, and $MnSO_4 \cdot H_2O$ (cationic ratio of Ni:Co:Mn = 6:2:2) solutions with a concentration of 2.0 mol L^{-1} were slowly dripped into a reactor under nitrogen atmosphere. At the same time, NaOH solution (4.0 mol L^{-1}) and NH_4OH solution (1.0 mol L^{-1}) as precipitation agent chelating agent (NaOH and NH_4OH with the mole ratio of 2:1) were separately added. The reaction temperature was kept at 50 °C and pH was controlled by NaOH solution to 11. The reaction was performed for 12 h to obtain $Ni_{0.6}Co_{0.2}Mn_{0.2}(OH)_2$ slurry, and the slurry was washed, filtered and dried at 110 °C. Secondly, layered $LiNi_{0.6}Co_{0.2}Mn_{0.2}O_2$ was synthesized by mixing stoichiometric of $Ni_{0.6}Co_{0.2}Mn_{0.2}(OH)_2$ precursor and 5 wt.% excess Li_2CO_3, then heating the mixture at 850 °C for 15 h in air.

Various mass ratio of TiO_2-coated $LiNi_{0.6}Co_{0.2}Mn_{0.2}O_2$ were prepared by a hydrolyzation method. Firstly, the calculated tetra-*n*-butyl titanate ($C_{16}H_{36}O_4Ti$) was dissolved in absolute ethanol, and then the pristine $LiNi_{0.6}Co_{0.2}Mn_{0.2}O_2$ power was added to the mixed solution. Subsequently, a mixed solution of ethanol and deionized water with the volume ratio of 2:1 was added into the suspension dropwise. Then the mixture was stirred at 25 °C for 4 h and continuously stirred at 60 °C to vaporize the solvent completely. Finally, the dried mixture was heated at 450 °C for 5 h in air with a 2 °C min^{-1} heating rate, and the TiO_2-coated $LiNi_{0.6}Co_{0.2}Mn_{0.2}O_2$ samples were obtained. The amounts of the coated TiO_2 were about 0.0, 0.5, 1.0, 1.5 and 3.0 wt.% of the $LiNi_{0.6}Co_{0.2}Mn_{0.2}O_2$ powders, respectively.

The X-ray diffraction (XRD, D/Max-2000) with Cu-Ka radiation was employed to identify the crystal structure of the powders in the 2θ range from 10 to 90° with a step size of 0.01° and a count time of 4 s. Scanning electron microscope (SEM, S-4800), transmission electron microscope (TEM, JEOL JEM-100CX) and high resolution transmission electron microscope (HRTEM, JEOL JEM-2100F) were used to observe the particle morphology of the powders and the status of coating layer. Energy dispersive spectroscopy (EDS) was obtained in conjunction with SEM to determine the element content of powders.

The electrochemical properties were performed using CR2032 coin-type cells. The electrode formulation consisted of 94.4 wt.% of active material, 3.1 wt.% of carbon black and 2.5 wt.% of polyvinylidene fluoride (PVDF) binder. Enough *N*-methyl-2-pyrrolidone (NMP) was added to form the slurry. The cathode was manufactured by coating the slurry on an aluminum foil followed by drying at 120 °C for 12 h in a vacuum oven and then being pressed with 20 MPa pressures. CR2032 coin-type cells were assembled in an argon-filled glove box, consisting of the as-prepared cathode, lithium foil anode, electrolyte: 1 M $LiPF_6$ dissolved in a mixture of EC–DMC(1:1 vol.%) and separator: Celgard-2400 microporous polypropylene membrane. The cells were measured using a Neware CT-3008W battery test system (Shenzhen, China) within the potential range between 3.0 and 4.5 V at different current densities. The electrochemical impedance spectroscopy (EIS) tests were performed using electrochemical workstation (CHI 660D) with a voltage of 5 mV amplitude over a frequency range from 10^5 Hz to 0.1 Hz. All the characterizations and measurements were conducted at room temperature.

Thermal stabilities of the pristine and TiO_2-coated $LiNi_{0.6}Co_{0.2}Mn_{0.2}O_2$ were studied using differential scanning calorimetry (DSC, NETZSCH STA 449 C). The assembled coin-type cells were first fully charged to 4.5 V at the rate of 0.2 C (28 mA g^{-1}) and then disassembled in an argon-filled glove box to obtain the electrodes. The electrolyte on the surface of the electrodes was removed and then the electrodes were dried under vacuum. The cathode materials were finally scraped from the dried electrodes, and then about 5 mg powers were hermetically sealed in the aluminum DSC sample pan. The DSC tests were performed from 100 to 350 °C with a heating rate of 10 °C min^{-1}.

3. Results and discussion

The XRD patterns of the pristine and TiO_2-coated $LiNi_{0.6}Co_{0.2}Mn_{0.2}O_2$ are presented in Fig. 1. All diffraction peaks from the XRD patterns are indexed on the basis of a hexagonal α-$NaFeO_2$ layered structure with space group R-3m without obvious impurities and secondary phase. The distinct splitting of (006)/(102) and (108)/(110) peaks for all samples demonstrates that these materials have a well-developed layered structure [5]. This suggests that the crystal structure of $LiNi_{0.6}Co_{0.2}Mn_{0.2}O_2$ is not affected by the TiO_2 coating. As is seen in Fig. 1(f), the obtained product is the anatase phase of TiO_2 with well ordered crystalline, which matches well with JCPDS card (78-2486). The absence of diffraction patterns corresponding to TiO_2 may be due to the small amount of TiO_2 coating [26].

Furthermore, the corresponding lattice parameters of all samples are calculated by the Rietveld refinement and listed in Table 1. By comparison, lattice parameters of the TiO_2-coated samples show no significant change, which implies that the TiO_2 is not incorporated into the $LiNi_{0.6}Co_{0.2}Mn_{0.2}O_2$ host structure and only coated on the surface of the core material. This conclusion is supported by SEM, TEM and EDS data presented in the following section. However, the intensity ratio of I_{003}/I_{104} is sensitive to the coating content. With increasing TiO_2 content, the I_{003}/I_{104} ratio increased firstly and then decreased. Among these samples, 1.0 wt.% TiO_2-coated $LiNi_{0.6}Co_{0.2}Mn_{0.2}O_2$ has the largest value of ratio of I_{003}/I_{104}, about 1.481. Generally, intensity ratio of I_{003}/I_{104} is always a sensitive parameter to determine the degree of cation mixing of the materials [27]. When the ratio is more than 1.2, the I_{003}/I_{104} ratio is higher, the degree of cation mixing is lower, and the materials have a good layered structure with small cation disorder and its

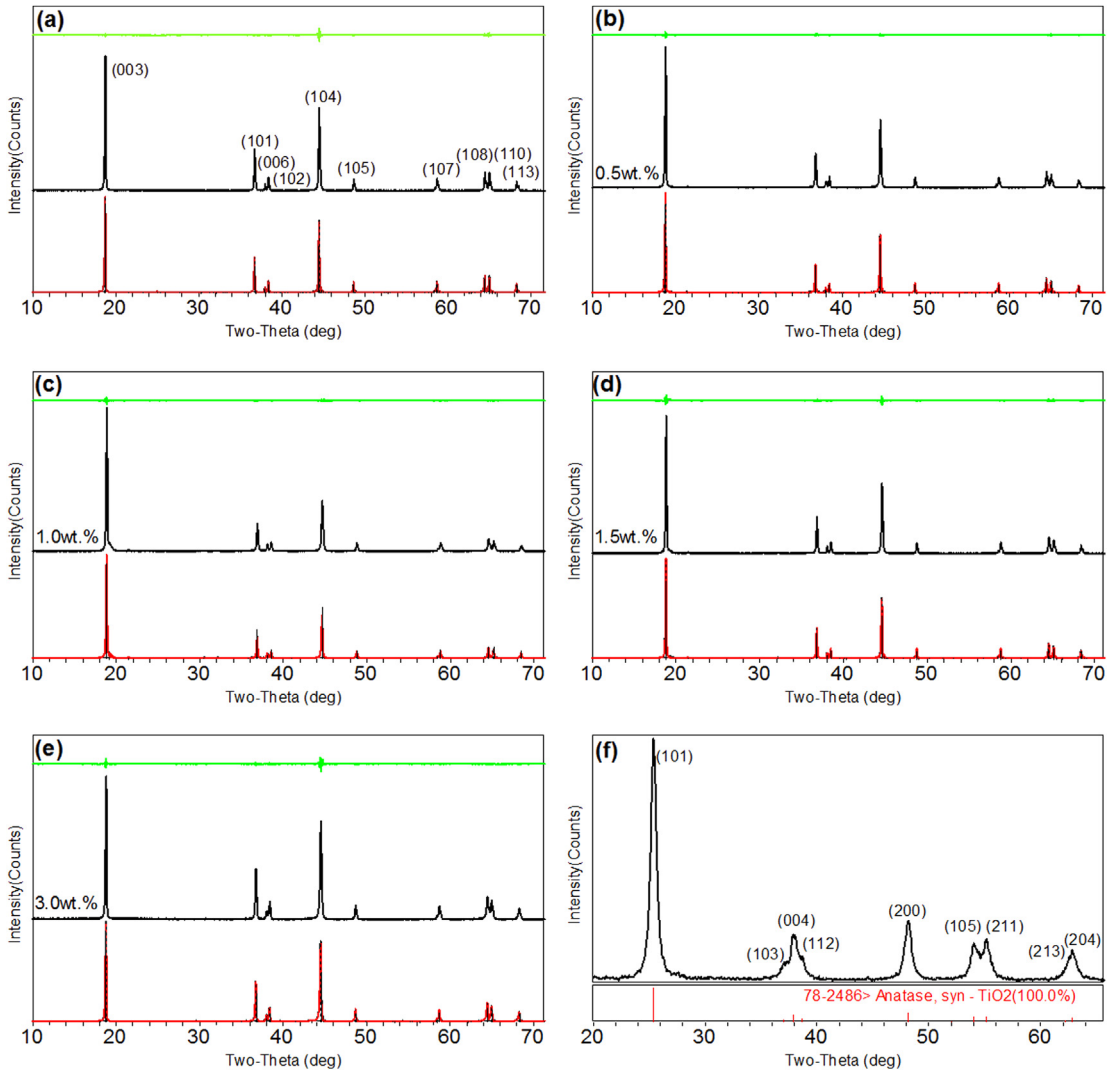

Fig. 1. XRD patterns: (a) pristine $LiNi_{0.6}Co_{0.2}Mn_{0.2}O_2$; (b) 0.5 wt.%; (c) 1.0 wt.%; (d) 1.5 wt.%; (e) 3.0 wt.%; (f) coating material.

electrochemical performance is relatively better [12,27]. Therefore, 1.0 wt.% TiO_2-coated $LiNi_{0.6}Co_{0.2}Mn_{0.2}O_2$ is expected to exhibit the best electrochemical performance.

SEM images of the pristine and TiO_2-coated $LiNi_{0.6}Co_{0.2}Mn_{0.2}O_2$ samples are shown in Fig. 2. It can be seen that the surface morphology of the powders is changed after coating. The pristine $LiNi_{0.6}Co_{0.2}Mn_{0.2}O_2$ particles are lamella in shape, and the surface of the particles is smooth with clear edge, as is clearly shown in Fig. 2(a). While the TiO_2-coated $LiNi_{0.6}Co_{0.2}Mn_{0.2}O_2$ particles become agglomerate, and the surface of the particles becomes rough. Among them, the 1.0 wt.% TiO_2-coated sample provides relatively more uniform particle size distribution and better dispersion. To identify the elements on the surface of the coated $LiNi_{0.6}Co_{0.2}Mn_{0.2}O_2$ powders, EDS has been carried out. As shown in Fig. 2(f), the presence of Ti elemental peaks after coating indicates that the TiO_2 coating layer is formed on the surface of the $LiNi_{0.6}Co_{0.2}Mn_{0.2}O_2$ powders successfully. The TEM images of the pristine and 1.0 wt.% TiO_2-coated $LiNi_{0.6}Co_{0.2}Mn_{0.2}O_2$ samples are shown in Fig. 3. By comparing Fig. 3(a) with (b), it can be seen that the surface of the $LiNi_{0.6}Co_{0.2}Mn_{0.2}O_2$ particle has formed a compact TiO_2 coating layer with thickness about 25–35 nm.

Table 1
Lattice parameters, c/a and I_{003}/I_{104} values of samples.

Samples	a/Å	c/Å	c/a	I_{003}/I_{104}
Pristine $LiNi_{0.6}Co_{0.2}Mn_{0.2}O_2$	2.8623	14.1785	4.954	1.235
0.5 wt.% TiO_2-coated	2.8625	14.1812	4.954	1.358
1.0 wt.% TiO_2-coated	2.8631	14.1793	4.952	1.481
1.5 wt.% TiO_2-coated	2.8653	14.1882	4.952	1.264
3.0 wt.% TiO_2-coated	2.8685	14.1871	4.946	1.165

To directly investigate the crystal structure of the coating material on the surface of the cathode material, high resolution transmission electron microscope (HRTEM) is employed. The HRTEM image of TiO_2-coated $LiNi_{0.6}Co_{0.2}Mn_{0.2}O_2$ is shown in Fig. 4. Two different lattice fringes can be seen in Fig. 4(b). The interplanar distance of 0.475 nm, corresponding to the (003) crystal plane, which represents the core material belonging to the hexagonal layered crystal structure. And the distance between the lattice fringe is 0.352 nm, corresponding to the (101) lattice plane, which is the typical characteristics of anatase phase of TiO_2 [28], and in accordance with the XRD pattern. The HRTEM image of TiO_2-coated $LiNi_{0.6}Co_{0.2}Mn_{0.2}O_2$ reveals that the crystal structure of the coating material is the anatase phase TiO_2.

Fig. 5 shows the initial charge and discharge profiles of the pristine and various amounts TiO_2-coated $LiNi_{0.6}Co_{0.2}Mn_{0.2}O_2$

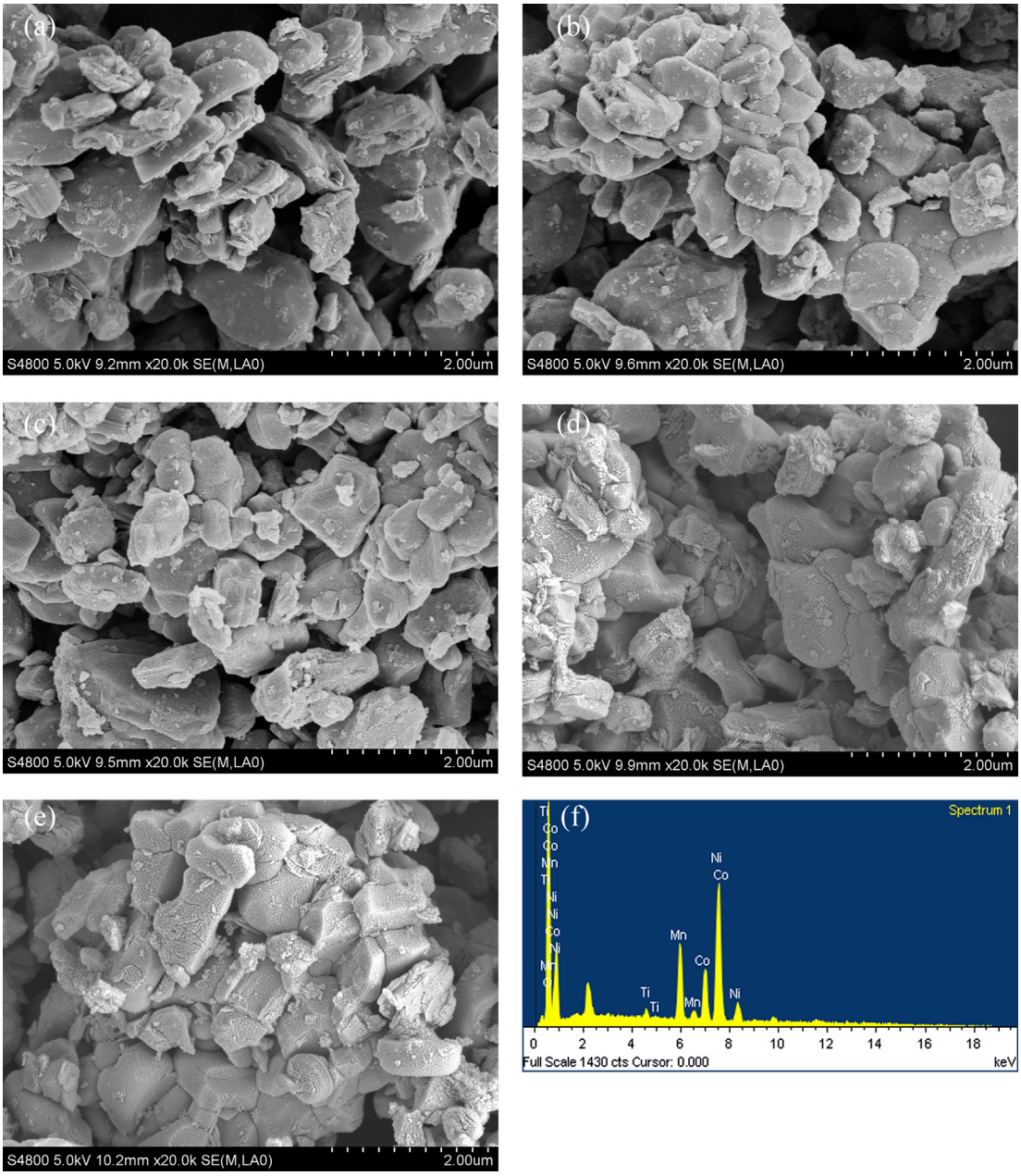

Fig. 2. SEM images of pristine and TiO_2-coated $LiNi_{0.6}Co_{0.2}Mn_{0.2}O_2$: (a) pristine; (b) 0.5 wt.%; (c) 1.0 wt.%; (d) 1.5 wt.%; (e) 3.0 wt.%; (f) EDS spectrum of 1.0 wt.% TiO_2-coated $LiNi_{0.6}Co_{0.2}Mn_{0.2}O_2$.

materials at current density of 0.2 C (28 mA g^{-1}) in voltage range of 3.0–4.5 V. All have stable and smooth voltage plateau in the initial charge/discharge process. And no distinct difference is observed in the initial charge/discharge process also indicates that the coating process cause no damage to the intrinsic electrochemical performance of the cathode material [26,29]. The initial charge/discharge capacities of the pristine $LiNi_{0.6}Co_{0.2}Mn_{0.2}O_2$ are 220.9 mAh g^{-1}/187.6 mAh g^{-1} and its initial coulombic efficiency is 84.9%. With increasing the content of TiO_2 coating, the discharge capacity and initial coulombic efficiency both increase firstly and then decrease. They are 195.4 mAh g^{-1}/88.7%, 193.9 mAh g^{-1}/89.8%, 188.5 mAh g^{-1}/89.3% and 174.8 mAh g^{-1}/85.3% respectively for 0.5, 1.0, 1.5 and 3.0 wt.% TiO_2-coated materials. Obviously, both the initial discharge capacity and coulombic efficiency of the pristine $LiNi_{0.6}Co_{0.2}Mn_{0.2}O_2$ can be enhanced by appropriate amount of TiO_2 coating. Theoretically, surface coating would not bring positive role on the discharge capacity of the cathode material due to the electrochemical inactive material of the TiO_2. However, the anatase TiO_2 coating will act as a mixed (electronic + ionic) conductor when Li is intercalated, and Li ions can easily move through the anatase lattice [30]. Meanwhile, the existence of the coating can suppress the interface reaction between the cathode and electrolyte, and then reduce the interface resistance and facilitate the Li^+ diffusion [7,29,31]. These conclusions are further confirmed by the EIS test later. In addition, the enhancement of the initial coulombic efficiency indicates that the ordering of the layered structure is increased by coating [32], which agrees well with the results of the XRD analysis. However, when the coating amount is up to 3.0 wt.%, the discharge capacity and initial coulombic efficiency decrease remarkably and the polarization increases apparently. This can be

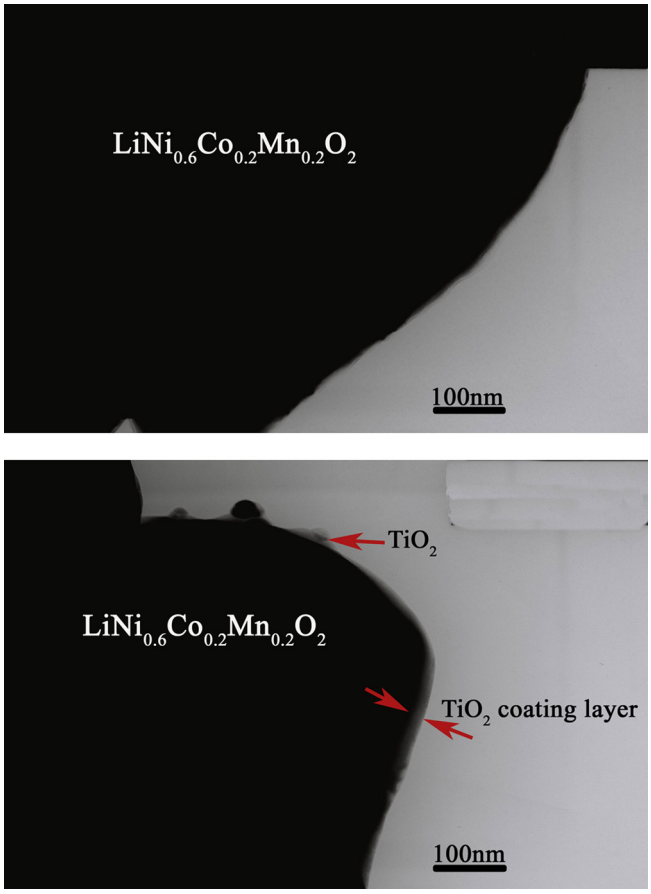

Fig. 3. TEM images of pristine and 1.0 wt.% TiO_2-coated $LiNi_{0.6}Co_{0.2}Mn_{0.2}O_2$ particles.

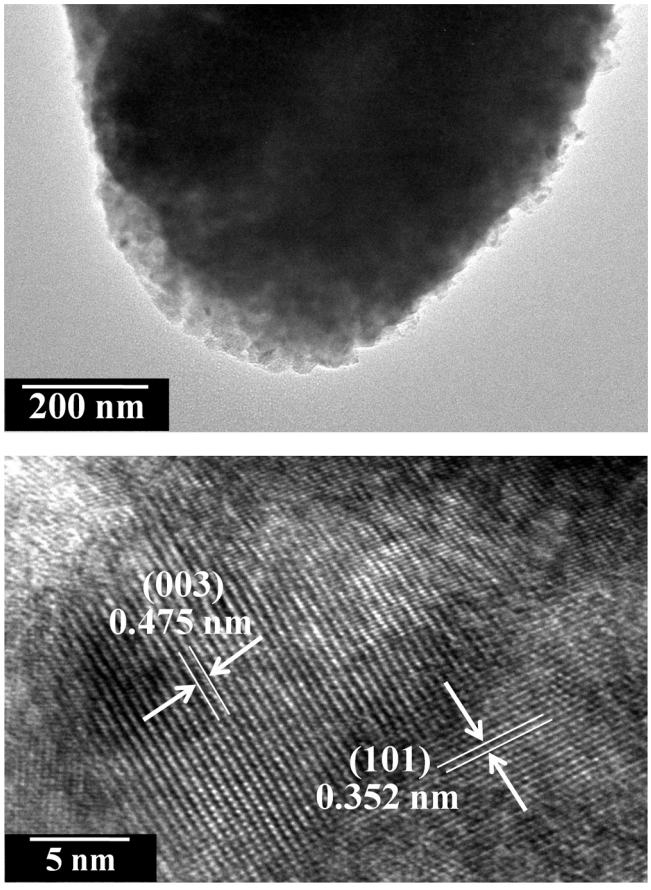

Fig. 4. HRTEM image of TiO_2-coated $LiNi_{0.6}Co_{0.2}Mn_{0.2}O_2$ particles.

caused by the excess inactive TiO_2 coated on the surface of $LiNi_{0.6}Co_{0.2}Mn_{0.2}O_2$, which forms an impedance and then effect on the intercalation and deintercalation of lithium ions [12,22].

The initial charge and discharge curves and cycling performances of the pristine and various amounts TiO_2-coated $LiNi_{0.6}Co_{0.2}Mn_{0.2}O_2$ materials at current density of 1 C (140 mA g^{-1}) in voltage range of 3.0–4.5 V are shown in Fig. 6(a) and (b). As shown, the pristine sample shows obvious capacity fade, from 175.1 mAh g^{-1} to 136.7 mAh g^{-1} after 50 cycles with capacity retention of only 78.1%. For the TiO_2-coated samples, the capacity retention of the $LiNi_{0.6}Co_{0.2}Mn_{0.2}O_2$ coated with 0.5, 1.0, 1.5 and 3.0 wt.% TiO_2 is 85.9, 88.7, 84.1 and 82.1% after 50 cycles, respectively. Obviously, the cycle performance of the cathode materials is improved by TiO_2 coating. Among them, the 1.0 wt.% TiO_2-coated $LiNi_{0.6}Co_{0.2}Mn_{0.2}O_2$ exhibits the best cycling performance and highest capacity of 157.3 mAh g^{-1} after 50 cycles. It demonstrates that appropriate amount of TiO_2 coating can obviously improve the cycling stability of $LiNi_{0.6}Co_{0.2}Mn_{0.2}O_2$ cathode materials. This is mainly attributed to the inert anatase TiO_2 coating, which protects the active material from reacting with the electrolyte and reduces the interfacial resistance between the cathode and the electrolyte [7,18,29]. However, excess amount (3.0 wt.%) of inert TiO_2 coating can negatively affect the materials, reducing the capacity and cyclic stability, which results from that the coating layer can reduce contact area between the active material and the electrolyte, and thus suppressing the transition of ions.

The rate capabilities of the pristine and TiO_2-coated $LiNi_{0.6}Co_{0.2}Mn_{0.2}O_2$ electrodes at various C-rates between 3.0 and 4.5 V vs. Li/Li^+ are presented in Figs. 7 and 8. The cells are firstly charged to 4.5 V at 0.2 C and then discharged at 0.2, 1, 2 and 5 C for every 10 cycles, respectively. With the increasing of the current density, the discharge capacity of the pristine and TiO_2-coated $LiNi_{0.6}Co_{0.2}Mn_{0.2}O_2$ electrodes all decrease due to polarization [7]. The discharge curves of the pristine and 1.0 wt.% TiO_2-coated $LiNi_{0.6}Co_{0.2}Mn_{0.2}O_2$ electrodes at various discharge rates over 3–4.5 V were shown in Fig. 7. It can be seen that the TiO_2-coated $LiNi_{0.6}Co_{0.2}Mn_{0.2}O_2$ electrode presents a better rate capability than the pristine one at various rates, especially at high C-rates. Moreover, the coated TiO_2-coated $LiNi_{0.6}Co_{0.2}Mn_{0.2}O_2$ shows a better cycling performance. For instance, in Fig. 7, the 1.0 wt.% TiO_2-coated

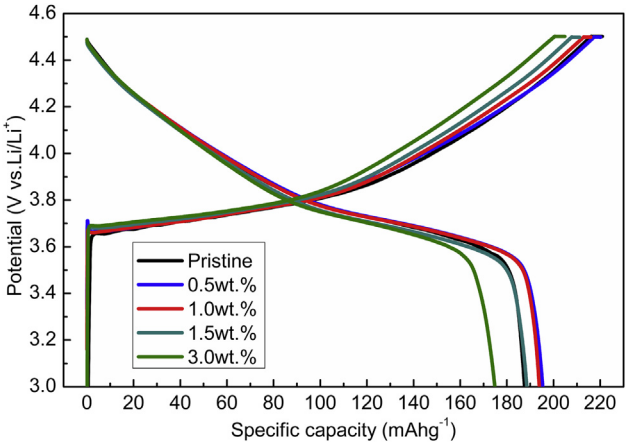

Fig. 5. Initial charge/discharge curves of the pristine and TiO_2-coated $LiNi_{0.6}Co_{0.2}Mn_{0.2}O_2$ electrodes at 0.2 C between 3.0 and 4.5 V.

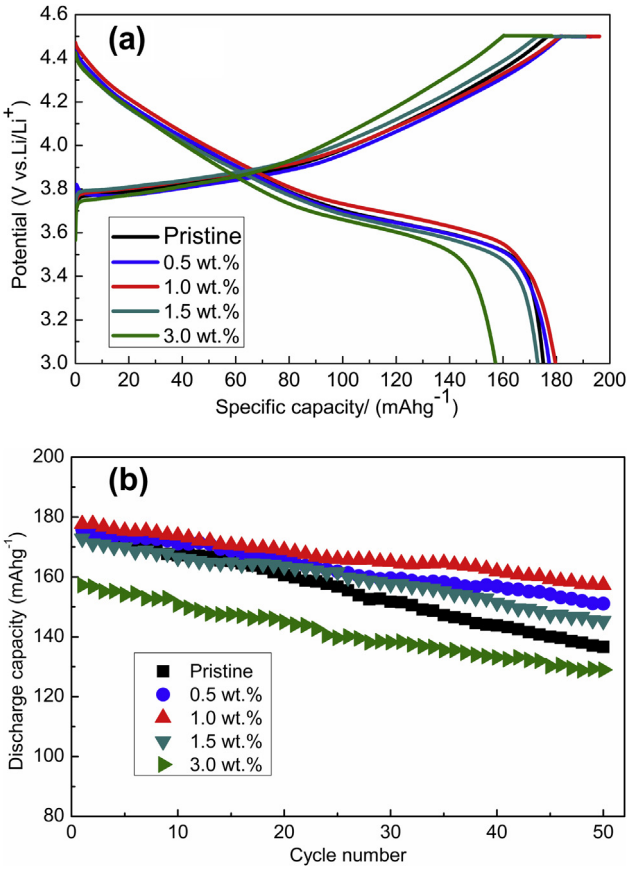

Fig. 6. Initial charge/discharge curves (a) and cycle performance (b) of pristine and TiO_2-coated $LiNi_{0.6}Co_{0.2}Mn_{0.2}O_2$ electrodes at 1 C over 3.0–4.5 V.

electrode shows a discharge capacity of 135.8 mAh g^{-1} after 10 cycles with capacity retention of 94.0% at 5 C rate, whereas the pristine electrode delivers a discharge capacity of only 85.4 mAh g^{-1} and poor capacity retention of 81.1% under the same conditions. Besides, it is interesting to note that the rate capability becomes even worse than the pristine one when the coating amount up to 3.0 wt.%. These results reveal that only proper amount of TiO_2 coating can improve the rate capability of the $LiNi_{0.6}Co_{0.2}Mn_{0.2}O_2$ electrode. According to the literature [2], there is a close correlation between cation disorder and rate capability in

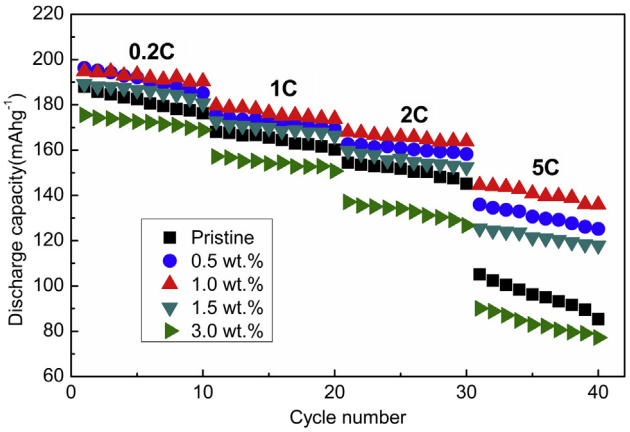

Fig. 7. Rate capability of the pristine and TiO_2-coated $LiNi_{0.6}Co_{0.2}Mn_{0.2}O_2$ electrodes at various discharge rates over 3–4.5 V.

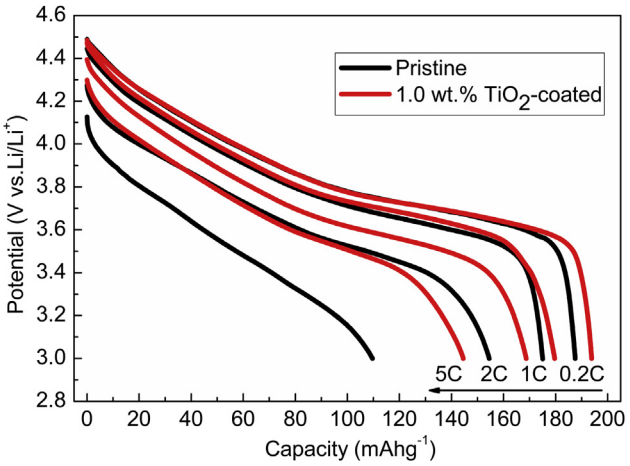

Fig. 8. Discharge curves of the pristine and 1.0 wt.% TiO_2-coated $LiNi_{0.6}Co_{0.2}Mn_{0.2}O_2$ electrodes at various discharge rates over 3–4.5 V.

the layered $LiNi_{1-y-z}Co_yMn_zO_2$ systems. Combining the results of XRD measurements, it can be speculated that the reduction of the cation disorder, the cathode/electrolyte interface instability and the polarization are important factors to the enhancement of the rate capability [7,12,33].

To further investigate the possible reason of improved electrochemical performance of the TiO_2-coated $LiNi_{0.6}Co_{0.2}Mn_{0.2}O_2$, electrochemical impedance spectroscopy (EIS) tests are performed for the pristine and 1.0 wt.% TiO_2-coated $LiNi_{0.6}Co_{0.2}Mn_{0.2}O_2$ electrodes after 30th and 50th cycles at 1 C between 3.0 and 4.5 V. Similar studies have also been reported in many cathode materials, such as AlF_3-coated $LiCoO_2$ [26], CaF_2 coated $LiMn_{1/3}Ni_{1/3}Co_{1/3}O_2$ [29] and Al_2O_3-coated $LiNi_{0.8}Co_{0.2}O_2$ [34]. As shown in Fig. 9(a), all

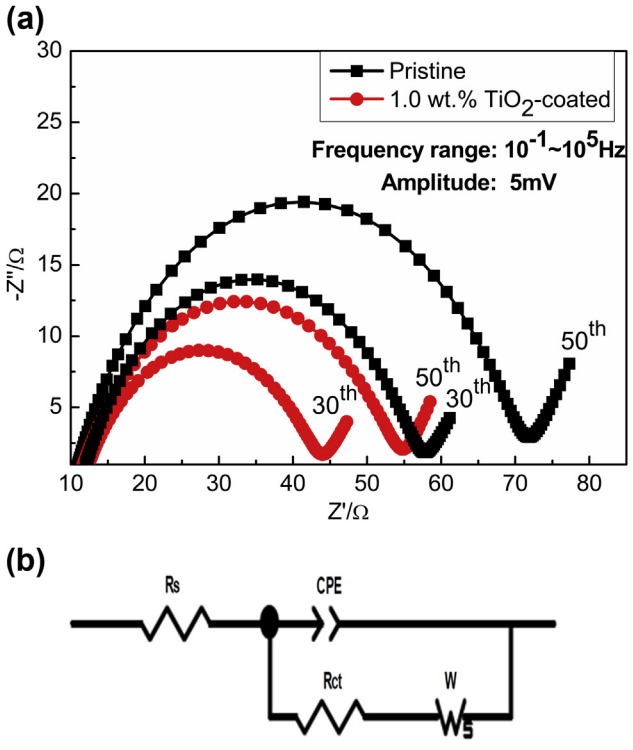

Fig. 9. Nyquist plots of pristine and 1.0 wt.% TiO_2-coated $LiNi_{0.6}Co_{0.2}Mn_{0.2}O_2$ (a); The equivalent circuit used to simulate EIS data (b).

impedance spectra can be distinguished in two sections: a semicircle at high frequency region and a sloping line at low frequency region. In general, each impedance spectra consists of three parts: a semicircle at high frequency region which represents resistance of surface film, the so-called solid electrolyte interface (SEI); another semicircle at the intermediate frequency region is related to the charge transfer resistance and interfacial capacitance in the electrode/electrolyte interface; and a sloping line at low frequency region is the Warburg impedance, which is associated with the lithium ions diffusion through the solid electrode [7,26,29,35]. The absence of a high frequency semicircle may be due to excellent rate performance (short diffusion path) or a small resistance offered by the surface layer for the migration of lithium ions which does not resist the diffusion of lithium ions [36]. An equivalent circuit, as shown in Fig. 9(b), is used to explain the impedance spectra. According to the literature [36,37], in this equivalent circuit, R_s represents the resistance of the electrolyte solution, R_{ct} corresponds to the charge transfer resistance, *CPE* is the capacitance of the electrode/electrolyte double layer, and *W* is the Warburg impedance. The values of the partial kinetic parameters for pristine and 1.0 wt.% TiO_2-coated $LiNi_{0.6}Co_{0.2}Mn_{0.2}O_2$ cells after 30th and 50th cycles are listed in Table 2. It can be seen that there is very little difference in solution resistance R_s between the pristine and TiO_2-coated $LiNi_{0.6}Co_{0.2}Mn_{0.2}O_2$ cells. This implies that the coated anatase TiO_2 is not dissolved into the electrolyte solution and thus changing the solution composition and affecting its conductivity [36]. However, the R_{ct} value changes quite apparent during cycling. The R_{ct} value of the pristine $LiNi_{0.6}Co_{0.2}Mn_{0.2}O_2$ cell at the 30th cycle is 46.55 Ω and it reached to 62.81 Ω at the 50th cycle, while the R_{ct} value of TiO_2-coated cell only increases from 31.88 to 44.78 Ω. Obviously, the R_{ct} of the 1.0 wt.% TiO_2-coated $LiNi_{0.6}Co_{0.2}Mn_{0.2}O_2$ is much smaller than that of the pristine one. According to the literature [7,18,23,29,31], it can be concluded that the anatase TiO_2 coating can suppress the interface reaction between the cathode and electrolyte and reduce the interface resistance. In addition, anatase TiO_2 coating on the cathode surface can decrease contact area between the active material and electrolyte and inhibit the cathode materials dissolution during cycling. Therefore, the improvement of the discharge capacity, capacity retention and rate capability for $LiNi_{0.6}Co_{0.2}Mn_{0.2}O_2$ should be attributed to the anatase TiO_2 coating.

The thermal instability of nickel-rich cathode materials, especially at the charged state, has always been a great disadvantage. Fig. 10 shows DSC profiles of the pristine and 1.0 wt.% TiO_2-coated $LiNi_{0.6}Co_{0.2}Mn_{0.2}O_2$ electrodes charged to 4.5 V versus Li. As can be seen in Fig. 10, the exothermic reaction peak temperature of the pristine $LiNi_{0.6}Co_{0.2}Mn_{0.2}O_2$ electrode is about 281 °C, but the TiO_2-coated $LiNi_{0.6}Co_{0.2}Mn_{0.2}O_2$ electrode shows a little higher exothermic peak temperature with 287.7 °C. Additionally, the exothermic peak area of the pristine $LiNi_{0.6}Co_{0.2}Mn_{0.2}O_2$ is much larger than that of the TiO_2-coated $LiNi_{0.6}Co_{0.2}Mn_{0.2}O_2$. The exothermic peak area signifies the amount of the oxygen generated from the decomposition of the cathode materials. Based on results above and according to the literature [10,18,22,25,38,39], the thermal stability of the $LiNi_{0.6}Co_{0.2}Mn_{0.2}O_2$ cathode material is enhanced attributed to the anatase TiO_2 coating, which can suppress the interface reaction between the electrode and electrolyte and stabilize the interface, resulting in reduction of the charge transfer resistance [4]. Moreover, the TiO_2-coated electrode has a higher exothermic peak temperature and a smaller exothermic peak area, indicating that the delithiated TiO_2-coated $Li_{1-x}Ni_{0.6}Co_{0.2}Mn_{0.2}O_2$ electrode can generate less oxygen during heating process, which reduces its decomposition at the charge state. This explains why the 1.0 wt.% TiO_2-coated $LiNi_{0.6}Co_{0.2}Mn_{0.2}O_2$ electrode has a better thermal stability charged at a high voltage.

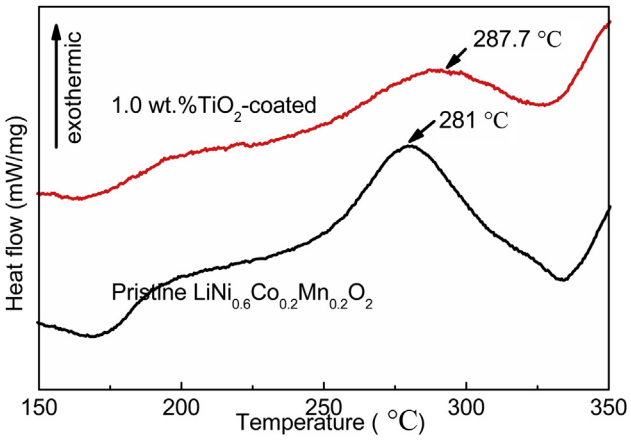

Fig. 10. DSC profiles of pristine and 1.0 wt.% TiO_2-coated $LiNi_{0.6}Co_{0.2}Mn_{0.2}O_2$ electrodes at charged state to 4.5 V.

Table 2
Values of the partial kinetic parameters for pristine and TiO_2-coated $LiNi_{0.6}Co_{0.2}Mn_{0.2}O_2$ cells after 30th and 50th cycles.

Samples	R_s/Ω	R_{ct}/Ω	
		30th cycle	50th cycle
Pristine	11.67	46.55	62.81
1.0 wt.% TiO_2	11.78	31.88	44.78

4. Conclusion

Nickel-rich layered $LiNi_{0.6}Co_{0.2}Mn_{0.2}O_2$ particles are coated with anatase TiO_2 nanoparticles. Appropriate amount of TiO_2 coated on the surface of $LiNi_{0.6}Co_{0.2}Mn_{0.2}O_2$ can significantly improve its discharge capacity, cycling stability and rate capability, even at a high cutoff voltage of 4.5 V. Especially, the 1.0 wt.% TiO_2-coated $LiNi_{0.6}Co_{0.2}Mn_{0.2}O_2$ electrode exhibits a capacity retention of 88.7% after 50 cycles at 1 C and shows a discharge capacity of 135.8 mAh g^{-1} after 10 cycles at 5 C, whereas those of the pristine electrode are only 78.1% and 85.4 mAh g^{-1}. Moreover, the 1.0 wt.% TiO_2-coated $LiNi_{0.6}Co_{0.2}Mn_{0.2}O_2$ electrode also shows a better thermal stability at the charged state. The improved electrochemical performance is mainly attributed to the following reasons: (1) the suppression of the interface reaction between the cathode and electrolyte, thus stabilizing the interface and reducing the impedance growth during cycling; (2) the prevention of the decomposition of the cathode materials, thereby enhancing the structural stability of the material.

Acknowledgment

Financial support by the National Basic Research Program of China (973 Program No. 2013CB934700) and The Innovation Fund for Technology Based Firm from Ministry of Science and Technology (No. 11C26215103354) are gratefully acknowledged.

References

[1] M.-H. Kim, H.-S. Shin, D. Shin, Yang-Kook Sun, J. Power Sources 159 (2006) 1328–1333.
[2] J. Choi, A. Manthiram, J. Power Sources 162 (2006) 667–672.
[3] T. Ohzuku, Y. Makimura, Chem. Lett. 30 (2001) 642–643.
[4] N. Yabuuchi, T. Ohzuku, J. Power Sources 119–121 (2003) 171–174.

[5] K.M. Shaju, G.V. Subba Rao, B.V.R. Chowdari, Electrochim. Acta 48 (2002) 145–151.
[6] B. Lin, Z. Wen, J. Han, X. Wu, Solid State Ionics 179 (2008) 1750–1753.
[7] F. Wu, M. Wang, Y.F. Su, S. Chen, B. Xu, J. Power Sources 191 (2009) 628–632.
[8] I. Belharouak, Y.-K. Sun, J. Liu, K. Amine, J. Power Sources 123 (2003) 247–252.
[9] Y.-K. Sun, Z.H. Chen, H.-J. Noh, H.-G. Jung, Y. Ren, S. Wang, C.S. Yoon, S.-T. Myung, K. Amine, Nat. Mater. 11 (2012) 942–947.
[10] H.-J. Noh, S.J. Youn, C.S. Yoon, Y.-K. Sun, J. Power Sources 233 (2013) 121–130.
[11] Y.-K. Sun, D.-H. Kim, H.-G. Jung, S.-T. Myung, K. Amine, Electrochim. Acta 55 (2010) 8621–8627.
[12] K. Yang, L.Z. Fan, J. Guo, X.H. Qu, Electrochim. Acta 63 (2012) 363–368.
[13] F. Wang, Y. Zhang, J.Z. Zou, W.J. Liu, Y.P. Chen, J. Alloys Compd. 558 (2013) 172–178.
[14] N.V. Kosova, E.T. Devyatkina, V.V. Kaichev, J. Power Sources 174 (2007) 965–969.
[15] J.G. Li, W. Li, Q. Zhang, X.M. He, J. Power Sources 189 (2009) 28–33.
[16] H. Cao, Y. Zhang, J. Zhang, B.J. Xia, Solid State Ionics 176 (2005) 1207–1211.
[17] P. Yue, Z.X. Wang, H.J. Guo, F.X. He, J. Solid State Electrochem. 176 (2012) 1823–1828.
[18] B.-C. Park, H.-B. Kim, S.-T. Myung, K. Amine, I. Belharouak, S.-M. Lee, Y.-K. Sun, J. Power Sources 178 (2008) 826–831.
[19] X.H. Xiong, Z.X. Wang, G.C. Yan, H.J. Guo, X.H. Li, J. Power Sources 245 (2014) 183–193.
[20] D. Ahn, J.-G. Lee, J.S. Lee, J. Kim, J. Cho, B. Park, Curr. Appl. Phys. 7 (2007) 172–175.
[21] D. Li, Y. Kato, K. Kobayakawa, H. Noguchi, Y. Sato, J. Power Sources 160 (2006) 1342–1348.
[22] R. Guo, P.F. Shi, X.Q. Cheng, L. Sun, Electrochim. Acta 54 (2009) 5796–5803.
[23] S.B. Jang, S.-H. Kang, K. Amine, Y.C. Bae, Y.-K. Sun, Electrochim. Acta 50 (2005) 4168–4173.
[24] H.S. Liu, Z.R. Zhang, Z.L. Gong, Y. Yang, Solid State Ionics 166 (2004) 317–325.
[25] Z.R. Zhang, J. Li, Y. Yang, Electrochim. Acta 52 (2006) 1442–1450.
[26] Y.-K. Sun, J.-M. Han, S.-T. Myung, S.-W. Lee, K. Amine, Electrochem. Commun. 8 (2006) 821–826.
[27] T. Ohzuku, A. Ueda, M. Nagayama, J. Electrochem. Soc. 140 (1993) 1862–1870.
[28] G. Cheng, M.S. Akhtar, O.-B. Yang, F.J. Stadler, Electrochim. Acta 113 (2013) 527–535.
[29] S.J. Shi, J.P. Tu, Y.J. Mai, Y.Q. Zhang, Y.Y. Tang, X.L. Wang, Electrochim. Acta 83 (2012) 105–112.
[30] B.V.R. Chowdari, G. Rao, S. Chow, J. Solid State Electrochem. 6 (2002) 565–571.
[31] J.M. Zheng, J. Li, Z.R. Zhang, X.J. Guo, Y. Yang, Solid State Ionics 179 (2008) 1794–1799.
[32] R.K.B. Gover, R. Kanno, B.J. Mitchell, J. Electrochem. Soc. 147 (2000) 4045–4051.
[33] Y.B. Lin, Y. Lin, T. Zhou, G.Y. Zhao, Y.D. Huang, Z.G. Huang, J. Power Sources 226 (2013) 20–26.
[34] G.T.-K. Fey, C.-Z. Lu, T. Prem Kumar, Y.-C. Chang, Surf. Coat. Technol. 199 (2005) 22–31.
[35] J.F. Xing, C.X. Chang, L.J. Yuan, J.T. Sun, Electrochem. Commun. 10 (2008) 1360–1363.
[36] K.C. Mahesh, H. Manjunatha, T.V. Venkatesha, G.S. Suresh, J. Solid State Electrochem. 16 (2012) 3011–3025.
[37] Y.-K. Sun, S.-W. Cho, S.-T. Myung, Electrochim. Acta 53 (2007) 1013–1019.
[38] B.J. Hwang, C.Y. Chena, M.Y. Chenga, R. Santhanama, K. Ragavendran, J. Power Sources 195 (2010) 4255–4265.
[39] J. Cho, B. Park, J. Power Sources 92 (2001) 35–39.